Catal Lett (2010) 138:187–192
DOI 10.1007/s10562-010-0387-z

Friedel–Crafts Hydroxyalkylation of Anisole Over Oxalic Acid Modified Hβ Zeolite

**Guoyi Bai · Haiyang Dou · Mande Qiu ·
Xinxin Fan · Fei He · Libo Niu · Zheng Ma**

Received: 3 March 2010 / Accepted: 2 June 2010 / Published online: 18 June 2010
© Springer Science+Business Media, LLC 2010

Abstract Oxalic acid modified Hβ (OA-Hβ) zeolite is found to have better catalytic performance than Hβ zeolite in the Friedel–Crafts hydroxyalkylation of anisole with chloral. This is attributed to the increase of weak and moderately-strong acid sites, caused by oxalic acid modification. Furthermore, it is believed that the carbonaceous deposits on the acid sites and the blockage of the pores, together with poisoning by chlorinated materials, are responsible for the deactivation of OA-Hβ zeolite, as indicated by NH_3-TPD, BET, SEM, TG and XPS measurement results. Moreover, partial regeneration of OA-Hβ zeolite can be achieved via subsequent calcination.

Keywords Hydroxyalkylation · Oxalic acid modification · Hβ zeolite · Stability · Deactivation

1 Introduction

Friedel–Crafts hydroxyalkylation of aromatic compounds by carbonyl derivates is of great industrial importance for the synthesis of commodities such as methylenedianiline and bisphenol A [1]. Presently, Friedel–Crafts hydroxyalkylation is carried out commercially using Lewis acids, such as $AlCl_3$, or mineral Brönsted acids, typically H_2SO_4. However, in view of the current environmental restrictions, there is an increasing demand for the replacement of conventional catalysts due to problems with disposal of spent catalysts, corrosion, toxicity and product isolation. Zeolites, with their unique acid properties and pore structures, are increasingly regarded as environmentally-friendly solid acid catalysts instead of traditional liquid acid catalysts in Friedel–Crafts type reactions [2–4]. Furthermore, acid modifications have been proven to be important for improving the activity of zeolites in these reactions [5, 6].

On the other hand, the selective synthesis of arylcarbinols directly from Friedel–Crafts hydroxyalkylation with aldehydes in the presence of zeolite is difficult because the arylcarbinol thus obtained can easily react with another aromatic compound to yield the corresponding bisarylalkane derivative under the same reaction conditions [7, 8]. Barthel and colleagues investigated the influence of zeolites and other reaction parameters on the hydroxyalkylation of aromatic compounds with chloral to furnish the arylcarbinol [9, 10], but few results have been reported on the stability of zeolite under hydroxyalkylation conditions.

In this paper, we report our recent studies on the effect of oxalic acid modification on the catalytic performance of Hβ zeolite in Friedel–Crafts hydroxyalkylation of anisole with chloral. The activity and stability of the oxalic acid modified Hβ zeolite were investigated and defined.

2 Experimental

2.1 Materials

All chemicals were of reagent grade and were used without further purification. The zeolites, Hβ (Si/Al = 25), ZSM-5

Electronic supplementary material The online version of this article (doi:10.1007/s10562-010-0387-z) contains supplementary material, which is available to authorized users.

G. Bai (✉) · H. Dou · M. Qiu · X. Fan · L. Niu · Z. Ma
College of Chemistry and Environmental Science, Hebei University, Baoding 071002, Hebei, People's Republic of China
e-mail: baiguoyi@hotmail.com

F. He
School of Chemical Engineering and Technology, Tianjin University, Tianjin 300072, People's Republic of China

(Si/Al = 38), MCM-41 (Si/Al = 25), HY (Si/Al = 4.5), were commercial samples purchased from Nankai University Catalyst Co., Ltd.

2.2 Catalyst Preparation

5.0 g Hβ zeolite was subjected to acid treatment by stirring with 20 mL oxalic acid (1.0 mol/L) at 50 °C for 1 h. After that, the samples were dried at 120 °C and then calcined at 550 °C for 5 h. The prepared zeolite was classified as OA-Hβ. Moreover, hydrochloric acid, tartaric acid, phosphoric acid and sulfuric acid modified Hβ zeolites were prepared in the same method and classified HA-Hβ, TA-Hβ, PA-Hβ, SA-Hβ, respectively.

2.3 Characterization of the Catalysts

X-ray diffraction (XRD) analysis was recorded on a Bruker D8 advance diffractometer with Cu Kα radiation. The BET surface area and total pore volume were determined using a Micromeritics Tristar II 3020 surface area and pore analyzer. Ammonia temperature-programmed desorption (NH_3-TPD) experiments were carried out in a TP-5000 instrument with a thermal conductivity detector. The surface acidity was monitored by FT-IR spectroscopy after adsorption of pyridine (Py-IR), using a Bruker Vector 22 spectrometer coupled to a conventional high vacuum system. The sample was compacted to a self-supporting wafer and was calcined at 400 °C for 1.5 h in an in situ IR gas cell under vacuum prior to pyridine adsorption. Pyridine was adsorbed at room temperature, and then the samples were heated to 200 °C and evacuated to remove physically adsorbed and weakly chemisorbed pyridine. The morphology of the samples was investigated using a JEOL JSM-7500 scanning electron microscopy (SEM) microscope. Thermogravimetric (TG) analysis was conducted on a NETZSCH QMS 403C TG/DSC/MS instrument in an argon gas flow. X-ray photoelectron spectroscopy (XPS) measurements were performed on a PHI 1600 spectrometer using a MgKα X-ray source for excitation.

2.4 Catalytic Tests

The hydroxyalkylation of anisole with chloral (Scheme 1) was carried out in a 50 mL round bottom flask equipped with a reflux condenser and a $CaCl_2$ tube. In a typical run, 40 mmol anisole and 40 mmol chloral were charged to the flask and heated to 40 °C. Then 1.0 g zeolite was added and the reaction continued at this temperature for 8 h with vigorous stirring. The OA-Hβ zeolite was isolated after the reaction by washing and drying at 120 °C. The regenerated OA-Hβ zeolite was obtained after calcination of the isolated OA-Hβ zeolite at 750 °C for 5 h. The reaction mixtures were analyzed by a gas chromatography using a 30 m SE-30 capillary column. The products were confirmed by GC–MS (Agilent 5975C) and ^{1}H NMR (Bruker Avance III 600 MHz).

3 Results and Discussion

3.1 Catalyst Selection and Characterization

As selection of a suitable catalyst is crucial for the efficient hydroxyalkylation of anisole, commercial zeolites were first examined in this reaction (Table 1, entries 1–4). It was found that Hβ zeolite was the most effective catalyst among them with an anisole conversion of 13.1% and a 1-(4-methoxyphenyl)-2,2,2-trichloroethanol (4-MPE) selectivity of 93.5%, accompanied by a trace of ortho-isomer. This can be attributed to the steric effect of the intermediate and product, consistent with the results discussed by Barthel [10]. A few bisaryl-product was detected as the main by-product. Considering the benefit of acid modification [5, 6], a series of acid-modified Hβ zeolites was prepared and investigated under the same reaction conditions (Table 1, entries 5–9). Just as we expected, some acid-modified zeolites, especially the OA-Hβ zeolite, exhibited higher activities than parent Hβ zeolite, the conversion of anisole catalyzed by OA-Hβ zeolite is nearly twice that of the Hβ zeolite. Thus, the OA-Hβ zeolite was chosen as the catalyst for further investigation and optimization.

Scheme 1

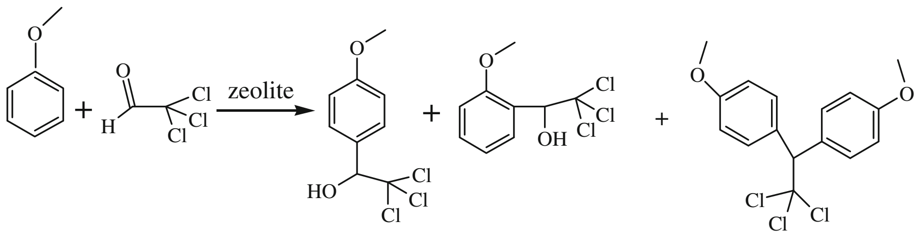

Table 1 Effects of different zeolites on conversion and chemoselectivity of the Friedel–Crafts hydroxyalkylation of anisole with chloral

Entries	Zeolite	Conversion of anisole (%)	Selectivity of 4-MPE (%)
1	MCM-41	9.3	88.8
2	ZSM-5	0.5	100
3	HY	7.1	79.1
4	Hβ	13.1	93.5
5	OA-Hβ	25.2	94.2
6	HA-Hβ	15.6	94.3
7	TA-Hβ	16.1	91.2
8	PA-Hβ	8.4	91.1
9	SA-Hβ	12.0	79.7

Reaction conditions—anisole: 40 mmol, chloral: 40 mmol, reaction temperature: 40 °C, catalyst amount: 1.0 g, reaction time: 8 h

The crystalline structure of Hβ and OA-Hβ zeolites are characterized by XRD, and XRD patterns are given in Fig. 1. The XRD patterns at 7.5° and 22.5° of OA-Hβ zeolite are weaker than that of Hβ zeolite. This suggests that the crystallinity of OA-Hβ zeolite decreases as a result of modification with oxalic acid, and this may favor the desired transformation.

N_2 adsorption and desorption results of Hβ and OA-Hβ zeolites are listed in Table 2. It was found that the OA-Hβ zeolite had higher BET surface area and pore volume than Hβ zeolite, possibly due to the dealumination of the zeolite after oxalic acid modification [11], which could result in production of more active sites for the reactants to adsorb and react, resulting in the observed higher activity of OA-Hβ zeolite.

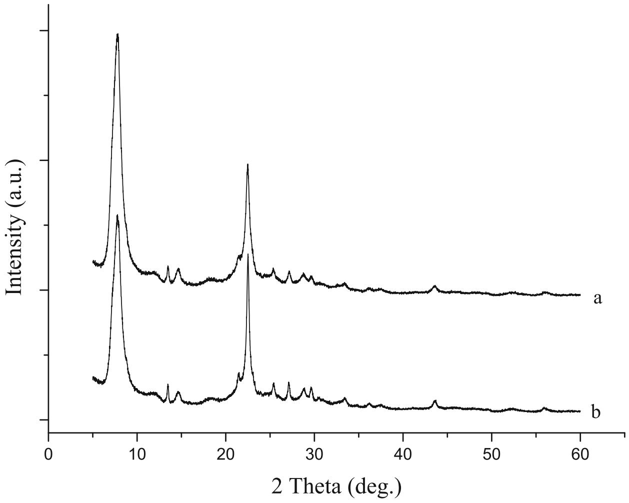

Fig. 1 XRD patterns of Hβ (**a**) and OA-Hβ (**b**) zeolites

Table 2 Textural properties of zeolites

Zeolite	BET surface area (m^2/g)	Pore volume (cm^3/g)
Hβ	331	0.26
OA-Hβ	408	0.30
Used OA-Hβ	13	0.05
Regenerated OA-Hβ	370	0.29

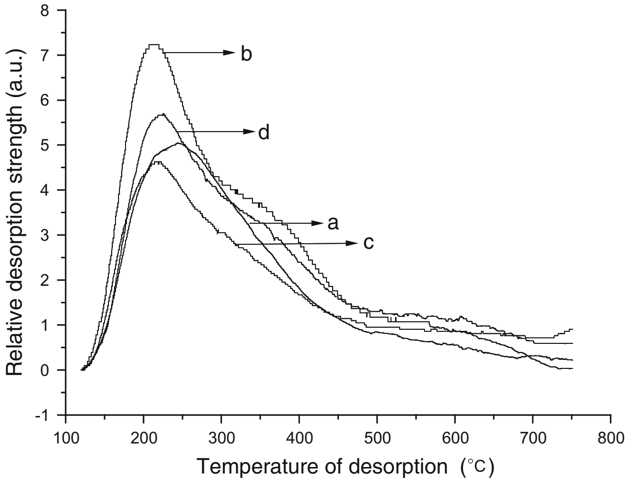

Fig. 2 NH_3-TPD profiles of Hβ (**a**), OA-Hβ (**b**), used OA-Hβ (**c**) and regenerated OA-Hβ (**d**) zeolites

NH_3-TPD profiles of Hβ and OA-Hβ zeolites are presented in Fig. 2 (curve a and b). The strong peaks centered at 180–260 °C are assigned to the weak acid sites in both zeolites and the peak centered approximately at 360 °C is assigned to the moderately-strong acid sites according to the literature [12]. It is clear that the amounts of both weak and moderately-strong acid sites in OA-Hβ zeolite are higher than those in Hβ zeolite. Thus, the catalyst activity appears to increase proportionally with the increase of the amounts of acid sites resulting from oxalic acid modification.

The results of Py-IR analysis of Hβ and OA-Hβ zeolites are listed Table 3. We conclude that OA-Hβ zeolite

Table 3 Acidic properties of Hβ and OA-Hβ zeolites from pyridine adsorption

Zeolite	Lewis[a]	Brönsted[a]	Total acidity[a]	L/B ratio
Hβ	12.27	2.38	14.64	5.16
OA-Hβ	17.01	0.64	17.65	26.41
Used OA-Hβ[b]	3.12	1.47	4.59	2.12

[a] Relative concentration

[b] The used sample was preliminary treated and then heated to remove pyridine both at 120 °C

contains more Lewis acid sites (1,450 cm^{-1}) than H*β* zeolite, while the amount of Brönsted acid sites (1,540 cm^{-1}) decreases remarkably after the oxalic acid modification. Therefore, the Lewis acid component of the zeolite promotes the conversion of anisole.

Table 4 Stability of OA-H*β* zeolite

OA-H*β* Zeolite	Conversion of anisole (%)	Selectivity of 4-MPE (%)
Fresh	79.0	93.7
Used	4.3	64.8
Regenerated 1st cycle	58.7	92.2
Regenerated 2nd cycle	48.1	94.7
Regenerated 3rd cycle	51.7	94.2
Regenerated 4th cycle	50.0	93.4
Regenerated 5th cycle	51.8	96.2
Regenerated 6th cycle	48.6	94.8
Regenerated 7th cycle	52.6	96.4
Regenerated 8th cycle	51.5	95.5

Reaction conditions—anisole: 40 mmol, chloral: 40 mmol, reaction temperature: 50 °C, catalyst amount: 5.0 g, reaction time: 8 h

3.2 Stability of OA-H*β* Zeolite

The preparation parameters of the OA-H*β* zeolite and the Friedel–Crafts hydroxyalkylation reaction parameters were both optimized to improve the activity of the catalyst. Finally, the stability of the optimized OA-H*β* zeolite was investigated under the optimum reaction conditions (Table 4). A marked deactivation occurs with the reused OA-H*β* zeolite with a conversion of anisole dropping from 79.0% in the first run to 4.3%. In contrast, on regenerating the re-isolated OA-H*β* zeolite after each run, the conversion of anisole first decreases to 58.7% and then stabilizes at about 50% in eight subsequent cycles all of which are better than the unmodified H*β* zeolite with a conversion of 30.9% under the same reaction conditions. Moreover, the selectivity for production of 4-MPE with the regenerated catalyst was retained at roughly 94%; whereas that of the re-isolated catalyst used without regeneration dropped to 64.8%. Therefore, the OA-H*β* zeolite shows enhanced activity and selectivity in this reaction in comparison with the unmodified H*β* zeolite as well as possessing the capacity for regeneration and recycling without loss of the

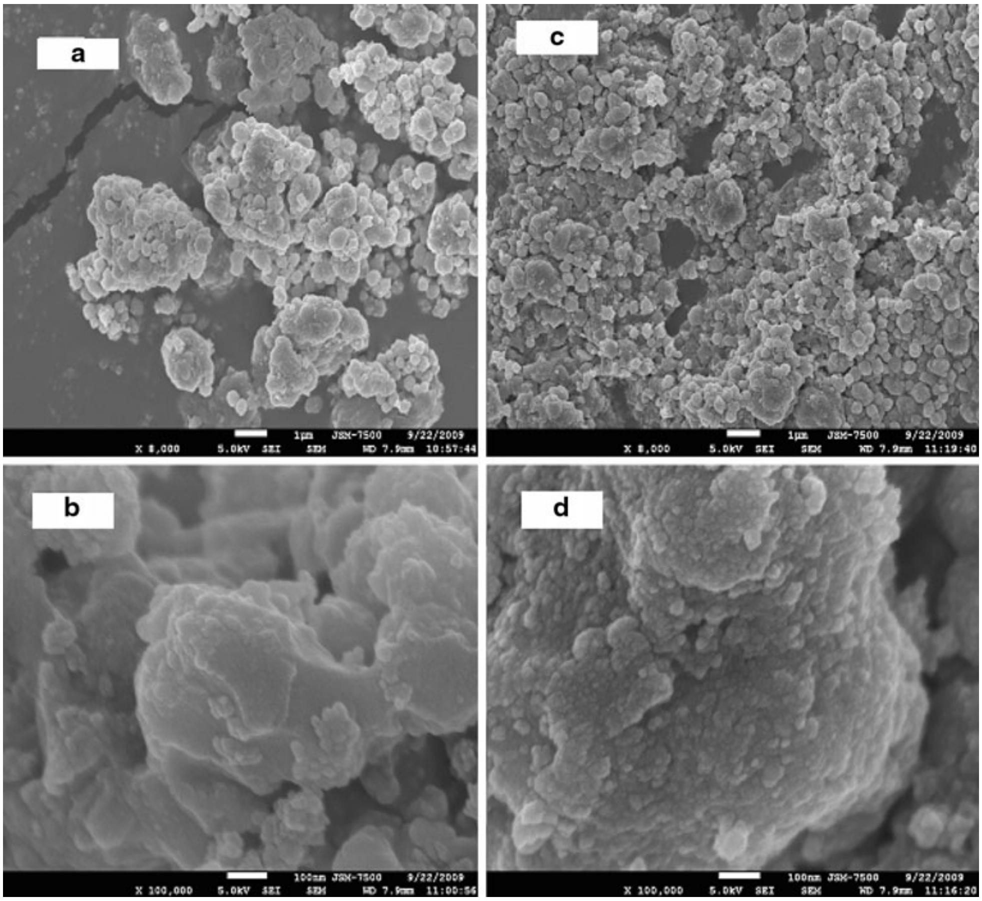

Fig. 3 SEM images of fresh OA-H*β* zeolite: **a** ×8,000 and **b** ×100,000; used OA-H*β* zeolite: **c** ×8,000 and **d** ×100,000

selectivity and retention of about two-thirds of its original catalytic activity.

In order to find the reason for the above results, the fresh, used and regenerated OA-Hβ zeolites were characterized and compared with the unmodified Hβ zeolite. As can be seen from Table 2, BET surface area and pore volume of the used OA-Hβ zeolite decrease remarkably to 13 m^2/g and 0.05 cm^3/g, which we propose to be caused by carbonaceous deposits on the surface and within the pores of the used OA-Hβ zeolite, and which are responsible for its deactivation [13]. SEM analyses on the fresh and used OA-Hβ zeolites show the differences directly (Fig. 3), with carbonaceous deposits detectable on the surface of the used OA-Hβ zeolite. Furthermore, the almost 17% weight loss of the used OA-Hβ zeolite and the detection of carbon dioxide in the gas phase, based on TG-MS, support this conclusion. Gratifyingly, the regenerated OA-Hβ zeolite has a relatively lower BET surface area (370 m^2/g) than the fresh one (408 m^2/g), but still higher than Hβ zeolite (331 m^2/g). We propose this to be due to the presence of irreversible carbonaceous deposition inside the pores, even after the regeneration by calcination.

XPS spectra of the used OA-Hβ zeolite also provide evidence for carbonaceous deposits on the surface, compared to the fresh and regenerated ones (Fig. 4), in total agreement with the BET and SEM results. On the other hand, chlorinated deposits are detected on the surface of the used OA-Hβ zeolite; whereas no chlorine is found on

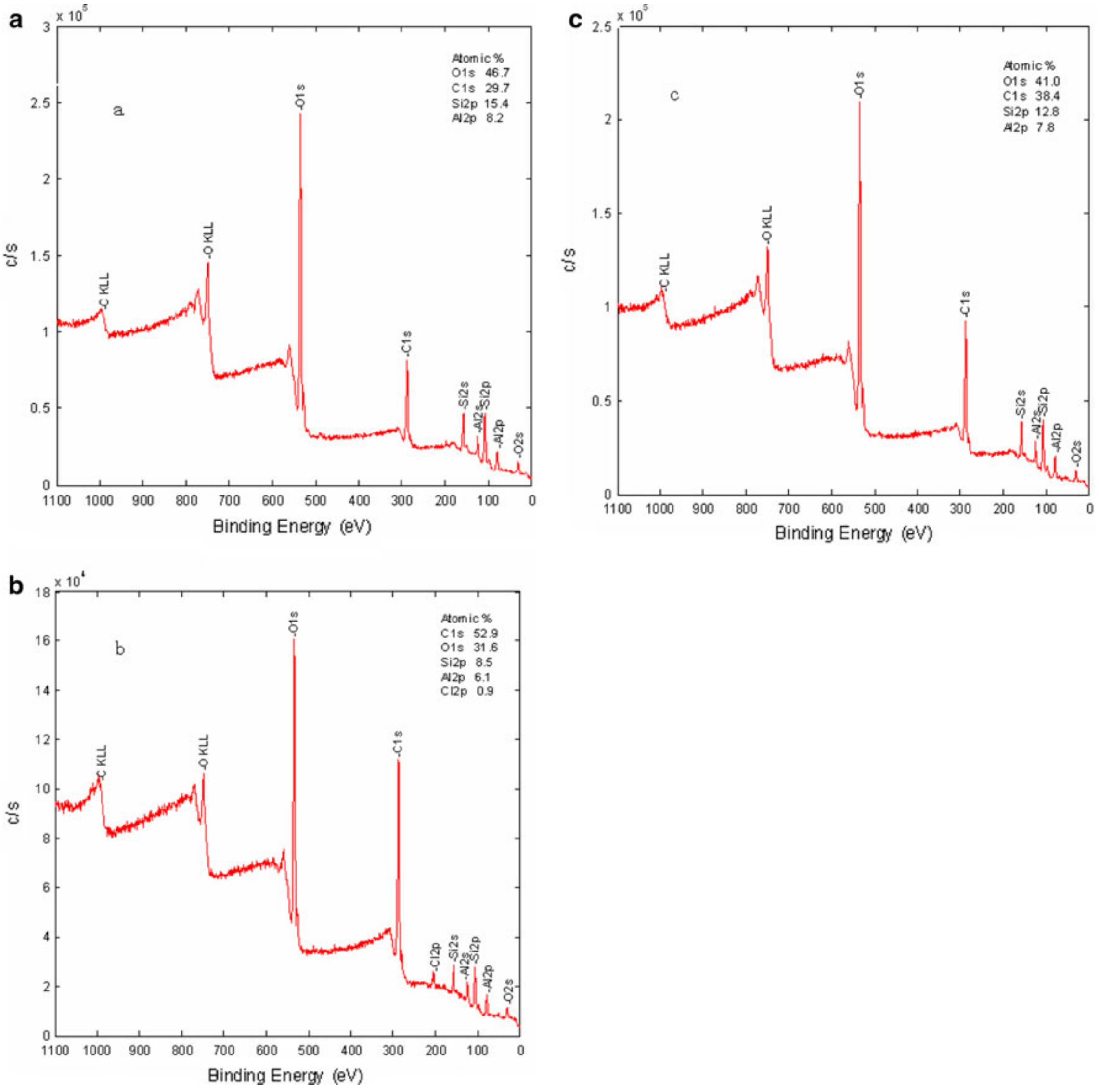

Fig. 4 XPS spectra of fresh OA-Hβ (**a**), used OA-Hβ (**b**) and regenerated OA-Hβ (**c**) zeolites

the surface of the regenerated one. We can thus deduce that the adsorption of chlorinated compounds may result in poisoning of a proportion of the Lewis acid sites, which further induces the catalyst deactivation.

The NH_3-TPD profile of the used OA-Hβ zeolite (Fig. 2, curve c) shows that the amount of acid sites decreases sharply, especially for the moderately-strong acid sites, compared to the fresh catalyst. However, the amount of weak and moderately-strong acid sites on the regenerated OA-Hβ zeolite only partially decreases (Fig. 2, curve d). Moreover, the amount of Lewis acid sites of the used OA-Hβ zeolite was also found to decrease significantly compared to the fresh OA-Hβ zeolite (Table 3). Thus, the decrease of acid sites due to carbonaceous deposition is believed to be the major source of deactivation.

4 Conclusions

The OA-Hβ zeolite, with a greater proportion of Lewis acid sites, exhibits better catalytic performance than Hβ zeolite in hydroxyalkylation of anisole, with an anisole conversion of 79.0% and a 93.7% selectivity of 4-MPE under the optimized reaction conditions. The increased weak and moderately-strong acid sites, as a result of modification by oxalic acid, are proposed to play an important role in this reaction. The carbonaceous deposits on the acid sites and their blockage of the zeolite pores are believed to be the reasons for deactivation of OA-Hβ zeolite. The adsorptions of chlorinated catalytic poisons onto the acid sites are proposed as another route for deactivation. Furthermore, partial regeneration of OA-Hβ zeolite with about two-thirds of the initial activity can be achieved reproducibly by burning off the carbonaceous deposits at 750 °C.

Acknowledgments The authors thank Professor L. M. Harwood for his assistance. Financial support by the National Natural Science Foundation of China (20806018), the Natural Science Foundation of Hebei Province (B2007000156), the Science Project of the Hebei Education Department (ZD200910) are gratefully acknowledged.

References

1. De Angelis A, Ingallina P, Perego C (2004) Ind Eng Chem Res 43:1169
2. Vinu A, Krithiga T, Gokulakrishnan N, Srinivasu P, Anandan S, Arige K, Murugesan V, Balasubramanian VV, Mori T (2007) Microporous Mesoporous Mater 100:87
3. Yuan B, Li ZS, Liu YJ, Zhang SS (2008) J Mol Catal A Chem 280:210
4. Song K, Guan JQ, Wu SJ, Yang Y, Liu B, Kan QB (2008) Catal Lett 126:333
5. Panneerselvam P, Thinakaran N, Thiruvenkataravi KV, Palanichamy M, Sivanesan S (2008) J Hazard Mater 159:427
6. Cheralathan KK, Kumar IS, Palanichamy M, Murugesan V (2003) Appl Catal A Gen 241:247
7. Botella P, Corma A, López-Nieto JM, Valencia S, Jacquot R (2000) J Catal 195:161
8. Sievers C, Liebert JS, Stratmann MM, Olindo R, Lercher JA (2008) Appl Catal A Gen 336:89
9. Barthel N, Finiels A, Moreau C, Jacquot R, Spagnol M (2000) Top Catal 13:269
10. Barthel N, Finiels A, Moreau C, Jacquot R, Spagnol M (2001) J Mol Catal A Chem 169:163
11. Zhao DS, Wang JL, Zhang J (2008) Catal Lett 126:188
12. Narender N, Krishna Mohan KVV, Kulkarni SJ, Ajit Kumar Reddy I (2006) Catal Commun 7:583
13. Corma A, García H (2000) J Chem Soc Dalton Trans 9:1381